Semi-Discrete Dynamical Model for Mountain-Front Recharge and Water Balance Estimation
(Rio Grande of Southern Colorado and New Mexico)

Christopher J. Duffy

Penn State University, University Park, Pennsylvania

Department of Civil and Environmental Engineering, Pennsylvania State University, University Park, Pennsylvania.

Abstract: This research is developing a distributed, dynamical model for estimating recharge and partitioning water budgets across the climatic and topographic gradients of the Rio Grande in southern Colorado and New Mexico. The present paper focuses on formulation of finite-volume balance equations and their physical basis; the relation of the model to qualitative characteristics of climate, vegetation and hydrogeologic conditions; and discretization of the model using the natural coordinates of the terrain. Explicit expressions are developed which link the upward and downward flux of water below the root zone (recharge and evapotranspiration respectively) to the water table position and the interaction of groundwater with ephemeral and perennial streamflow. The modeling strategy, originally proposed by Duffy (1996) for soil moisture and groundwater flow at the hillslope scale, is extended here to the case where major changes in terrain, climate, vegetation and hydrogeologic conditions require a distributed, but low-dimensional, water balance. The complexity or dimension of the model is determined by the choice of support scale of the geospatial data (e.g. terrain, climate, landuse, and vegetation features) and the corresponding relation of the subsurface contributing area to surface streams or ephemeral channels. The model approach is based on a semi-discrete finite volume method, where the partial differential equations are formed in terms of a coupled system of nonlinear ordinary differential equations. The model is demonstrated for a mountain-front setting in central New Mexico, the Llano de Sandia. A simulation scenario explores the long range impacts of abrupt climate change on upland recharge and riparian evapotranspiration through gains and losses of groundwater to the Rio Grande.

Preprint: AMERICAN GEOPHYSICAL UNION MONIOGRAPH

RECHARGE AND VADOSE-ZONE PROCESSES:
Alluvial Basins of the Southwestern United States

In press February 2004

INTRODUCTION

Modeling the response of large river basins to atmospheric forcing generally proceeds from one of two modeling strategies, each having distinctly different objectives. The first approach uses fully-discrete, numerical solutions to partial differential equations for energy, mass and momentum transport, where the discretization is over 4-D space-time domain. In this case the requirement of high-resolution spatial forecasts of hydrologic states (e.g. snow and soil moisture fields, water table surfaces, etc.) and the distribution of fluxes from recharge and baseflow, effectively determines the scale of the computation. A second strategy applies spatially- averaged equations for the purpose of estimating a dynamic water balance over a specidfied scale (Duffy, 1996; Bierkens, 1998). This approach responds to the needs of the modeler/manager for simulation of system-wide water budgets.

This paper explores a third strategy that combines elements of both modeling strategies. The approach is referred to as a "semi-discrete" method, where the model equations are discrete in space and continuous in time. The approach uses an integral form of the conservation equation and a finite volume discretization of space. The state variables are approximated by grid-cell averages. This leads to a system of ordinary differential equations in time, which are solved using higher order ODE methods. The method has the advantage of allowing the modeler to make a relatively coarse-grain representation of the river basin for the purpose of evaluating regional water budgets, while allowing lateral exchange and coupling with adjacent elements or HRU's (hydrologic response units). In the limit of small grid cells, the approach represents a high-resolution approximation to the original contiuum model. In this paper, a water balance is formed for a coarse-grain representation of the domain; while the multi-scale aspects of the model are developed elsewhere (Qu and Duffy, 2004). The goal of the research is to develop a GIS-based multi-scale strategy for modeling recharge and large-scale water budgets over complex terrain. The approach attempts to maintain the physical basis of the subsurface parameters, states and fluxes, while offering an adaptive strategy for dynamic water budget estimation within a conceptual modeling framework. Application of the approach to the Rio Grande in central New Mexico, serves to motivate general questions about modeling the water balance of large river basins such as: How does the physical landscape (topography, hydrostratigraphy, soils, vegetation, etc.) partition the water budget into the dominant modes of recharge within the basin? What is the linkage between diffuse or areal recharge and focused recharge from channels? What is the impact and time scales of climate change on mountain-front water resource systems?

THE PHYSICAL CONCEPTUAL FRAMEWORK

From the point of view of the water cycle, the Rio Grande basin, from the headwaters in the San Juan Mountains of southern Colorado to the southern New Mexico border at El Paso Texas, represents a critical water resource for sustaining municipal, agricultural, ecological and industrial water needs of this semi-arid region. A brief discussion of the hydroclimatic conditions across the basin serves to emphasize the large-scale coupling and importance of the basin conceptual hydrology to understanding long-term memory of the system.

Within the Rio Grande basin, spring and early summer runoff is dominated by high elevation winter snowpack accumulation and meltwater, while the late-summer monsoon brings thunderstorms which regulate the magnitude of the seasonal drought conditions at lower elevations (July to September). Both of these seasonal climate patterns are extremely variable in producing soil moisture, recharge and runoff over the complex terrain of the basin. For example, seasonal modes of atmospheric moisture are modulated on longer time scales by interannual, decadal and lower frequency oscillations reflecting larger scale ocean, atmosphere, and orbital oscillations. Land-use and land-cover changes will also have impacts on long time scales.

The "hydrologic conceptual model" forms the basis for defining local characteristics of the fluid storage volume and flux within a hydrologic contributing area and an associated river reach. The dynamical model proposed here is constructed by integrating the local conservation equation over the estimated physical storage volumes of the surface-groundwater regimes using the natural coordinates of the topography and the estimated vertical structure of the subsurface. In this way, the multidimensional local conservation equations in physical space are transformed to a lower-dimensional state space, where a practical number of ordinary differential equations need to be solved. The strategy is to decompose the river basin into sub-basins or hydrologic response units using natural coordinates of the terrain (elevation contours and watershed divide). Thus the volume element is formed by vertical projection of pairs of topographic contours and flow paths.

Forming the Hydrologic Conceptual Model.

The Upper Rio Grande flows extends from the headwaters in the San Juan Mountains of southern Colorado to the international boundary at El Paso Texas. The mountain and basin terrain is conveniently described with a conceptual model based on the characteristic hydrogeology, ecology, topography and climate conditions. Figure 1 illustrates the basin and the location of a mountain-front system, the Llano de Sandia, which extends from Albuquerque NM in the north to San Acacia NM in the south. The unit is bounded on the west by the Rio Grande, and the eastern edge is formed by the north-to-south trending Manzano and Los Pinos mountains. The elevation ranges from ~3050 m amsl at the highest point in the Manzano mountains, 2347 m at the highest point in the Los Pinos mountains, and 1420 m at the San Acacia gaging station and outlet to the region. The surface and subsurface hydrologic conditions along a typical cross-section is shown in Figure 2 (modified from Spiegel ,1955). The cross section is in the southern part of the Llano de Sandia (see Figure 1) and passes through the Sevilleta Long Term Ecological Research facility (http://sevilleta.unm.edu/).

Figure 1. Rio Grande basin from southern Colorado to El Paso Texas. The Llano de Sandia mountain-front system is shown in central New Mexico is shown in the figure.

The important point for this discussion is that there are three distinct zones across this topographic gradient, where conditions for recharge and storage of soil and groundwater are substantially different. Although distinct, these zones, described below, are clearly linked by hydrologic conditions above and below the land surface, and through climate and vegetation changes. The impact of these linkages on large-scale, coupled water budgets is examined later in this paper.

The conceptual hydrogeology of Spiegel (1955) suggests that the mountain uplands have shallow or perched water table conditions, with thin soils and residuum on crystalline fractured bedrock. Springs and intermittent streams are also observed. On the western mountain front, deep alluvial fans of the

Tertiary Santa Fe formation overlie buried fault blocks. The gently sloping llanos or erosional surfaces are cut on the Santa Fe formation and are veneered by pediment gravels and residuum. The latter is undifferentiated here. The piedmont alluvial plain and underlying alluvial fans or bajadas represent a zone of transmission losses by ephemeral channels and arroyos that cross the region. The water table is deep (60-300 m or more) below the llano and the likelihood of significant diffuse recharge is low. Within the floodplain of the Rio Grande, Quaternary alluvium deposits with depths of ~30-50 m overlie the Santa Fe formation. The depth to water table is generally shallow in the alluvium (0-5 m). Within the Rio Grande corridor, diffuse recharge is very low but the shallow water table is affected by upward flow from direct evaporation and transpiration of phreatophytes (J. Weiss, et al, 2004). Channel losses or gains from groundwater are evident along this reach of the Rio Grande, and ephemeral streams are a source of recharge.

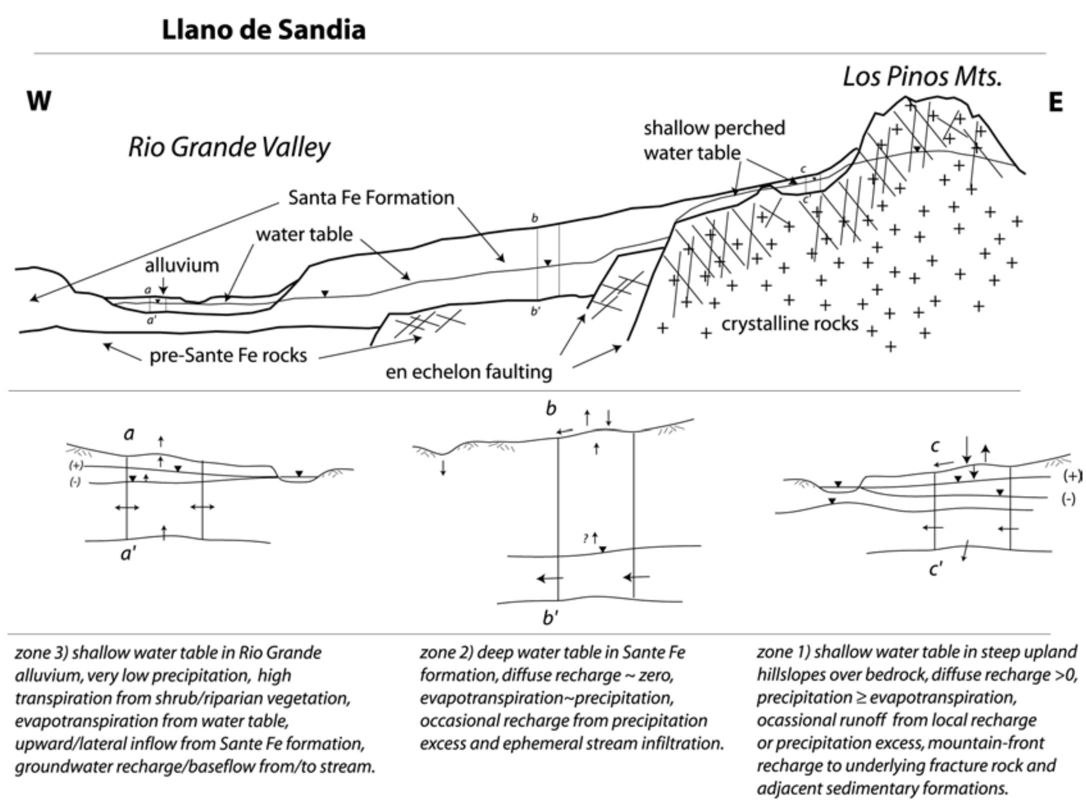

Figure 2. The hydrologic conceptual model for a section of the Llano de Sandia, located through the Sevilletta Long Term Ecological Research Center. Hydrogeology is adapted from Spiegel (1955). The profile indicates the three "similarity zones" where geology, climate, vegetation and water table conditions are distinct.

According to scientists of the Sevilletta LTER, the vegetation of this region represents a transition zone for major North American biomes, including Great Plains Grassland, Chihuahuan Desert, Great Basin Shrub-Steppe, Interior Chaparral, Mogollon (Pinon-Juniper) Woodland, and Montane Forests. Muldavin et al (1998) have constructed vegetation maps that identify montane woodlands of pinion and shrub oak in the mountainous areas of the Los Pinos mountains. Desert shrub (creosote, saltbush) and grasslands (grama and galleta) intermix at lower elevations on the gently sloping llano. Within the Rio Grande corridor and adjacent arroyos, riparian woodlands of cottonwood, salt cedar and russian olive predominate.

The annual temperature and precipitation of the region can be characterized by cold winters, generally dry from October to November with variable snow accumulations at higher elevations from December to March. The spring and early summer is hot, dry and windy; while late summer has a monsoon with significant thunderstorm activity. The monsoon is variable, but important to soil moisture and vegetation during the summer drought. Intense summer thunderstorms may contribute to ephemeral channel runoff and recharge; while winter precipitation is more likely to support diffuse recharge. Annual precipitation may exceed 50 cm/yr at the highest parts of the Los Pinos mountains to < 20 cm/yr in the Rio Grande valley.

A fundamental question for low elevation parts of a mountain-front system, is whether recharge occurs at all. This general point was raised by Phillips (1994) and more recently in a dissertation by Walvoord (2002). Their research suggests that conditions of low rainfall, high potential evaporation and the transpiration efficiency of desert shrubs across the southwest may actually create conditions where no recharge and small upward flow is the normal state. Furthermore, this condition may have existed since the end of the Pleistocene. From the perspective of a geochemical balance, Plummer et al. (2000) suggest that the Middle Rio Grande basin, which includes the Llano de Sandia, may have limited recharge or at least highly variable recharge related to ephemeral channel losses.

A corollary to the existence of recharge in arid basins is the concept that all water that moves below the root zone becomes recharge. If long term conditions support a slow upward flow (e.g hyperarid conditions with a deep water table), then even very wet periods of sustained precipitation and infiltration are unlikely to produce diffuse recharge as the equilibrium or average condition of upward flow is re-established. A related question is: What are the controls exerted by the physical environment on precipitation, evapotranspiration and recharge across an elevation gradient. The long term balance of precipitation less evapotranspiration, where $p\text{-}e_t$ is positive in upland regions and negative on the valley floor suggests that water budgets across the region are coupled and cannot be viewed in isolation. Clearly, the likelihood of recharge depends on the mean and variability of climate, soil, vegetation, and geologic conditions, with altitude playing an important role.

In the Los Pinos mountains $p\text{-}e_t>0$, likely supports diffuse recharge. On the piedmont alluvial plain, $p\text{-}e_t$ may be zero to slightly negative, and within the Rio Grande corridor $p\text{-}e_t<0$ is the most reasonable assumption. We can see that the conceptual model helps to clarify the basic relationships of the water balance in a mountain-front setting, and suggests the essential dimensions of the model. However, this analysis does not tell us about the time scales and dynamics of changing climatic conditions on recharge. To do this requires a coupled model approach to semiarid water budgets which is developed next.

Regional Water Balance as a Dynamical Model

A local, dynamic water balance can be formed by direct integration of the local conservation equation for a specified volume of unsaturated and saturated moisture storage. The control volume is defined by the natural coordinates of the terrain $dV=dzdA$,where z is elevation and dA is defined as a projected increment of area. In this paper, the area elements are formed by elevation contours and the bounding topographic flow paths or divide (Duffy, 1996). The integration is carried out over both the unsaturated and saturated volumes where the sense of the integration changes from a predominantly 1-D vertical flow regime in the unsaturated zone, to a 2-D lateral flow below the water table given by:

$$\int_A \int_h^{z_s} \left(\frac{\partial \theta}{\partial t} + \nabla \cdot q\right) dz dA = 0$$
$$\int_A \int_{z_b}^{h} \left(\frac{\partial \theta}{\partial t} + \nabla \cdot q\right) dz dA = 0 \qquad (1)$$

θ(z)s the vertical variation in moisture content, q is the Darcy flux velocity. The vertical control volume with surface area A is partitioned into complementary volumes above (+) and below the water table (-):

$$dV^+ = dzdA^+ \rightarrow (z_s - \phi)A^+$$
$$dV^- = dzdA^- \rightarrow (\phi - z_b)A^- \qquad (2)$$

The area increment dA is defined as the projected area associated with the vertical element dV. As shown in Figure 3, z_s , ϕ and z_b are the land surface, water table height and bedrock elevation respectively. From (2) the volume is first integrated over the depth of the aquifer. Making use of the Reynolds transport theorem (Duffy, 1996) and the divergence theorem in (1) to form the terrain-integrated dynamical model:

$$\sigma \frac{d}{dt} \int_A \zeta dA = \int_A q \cdot n dA - \int_A (q - \theta^+ u) \cdot n dA \qquad (3a)$$

$$\sigma \frac{d}{dt} \int_A \phi dA = \int_A (q - \theta^+ u) \cdot n dA - \int_\Gamma (\phi - z_b) q \cdot n d\Gamma \qquad (3b)$$

The first integral on the right hand side of (3a) is the net vertical infiltration to the soil column at the land surface, and the second term is the net vertical flux to/from the water table (recharge). n is the unit outward normal directed upward at the land surface and water table, and horizontally with respect to the vertical sides of the element for lateral groundwater flow. The recharge term at the free surface, depends on the flux q approaching/leaving the free surface boundary, and the velocity u of the water table itself. θ^+ and θ^- are the moisture contents as one approaches the water table from above or below respectively. The net horizontal volumetric flux of groundwater below the water table is given by the line integral:

$$\int_{\Gamma^-} (\phi - z_b) q \cdot n d\Gamma$$

Recall that Γ and A are projections of the control volume and the control volume boundary in the horizontal plane, respectively. After vertical integration, the point averages of moisture storage above and below the water table are respectively:

$$\zeta(x,y,t) = \int_h^{z_s} \frac{\theta - \theta_r}{\theta_s - \theta_r} dz,$$
$$\phi(x,y,t) = \int_{z_b}^{\phi(x,y)} \phi dz \qquad (4)$$

The quantities θ_r and θ_s are the residual and saturated soil moisture fraction respectively, and σ is the effective porosity. The model with volume-averaged states can now be expressed in semi-discrete form, that is, continuous in time and discrete space:

$$\left[\sigma_i \frac{d\zeta_i}{dt} = q_i^+ - q_i^0\right] A_i$$
$$\left[\sigma_i \frac{d\phi_i}{dt} = q_i^0 - q_i^-\right] A_i \qquad (5)$$
$$\sigma_i = \theta_s - \theta_r$$

where the vertically-averaged state variables (4) are now averaged over the projected area A_i:

$$\bar{\zeta}_i(t) = \frac{1}{A_i} \int_{A^+} \zeta(x,y) dA;$$
$$\bar{\phi}_i(t) = \frac{1}{A_i} \int_{A^-} \phi(x,y) dA \qquad (6)$$

and the soil moisture and saturated states become volume-averages. The flux rates (q^{+}, q^{-}, q^{o}) are themselves vector quantities which represent the various inputs and outputs, in units of volumetric flow per unit projected surface area

$q^{+} \Rightarrow$ vertical fluxes above the water table
$q^{o} \Rightarrow$ flux at the water table
$q^{-} \Rightarrow$ horizontal flux below the water table

To review, the basic model (5) is formed by integration over the projected flow volume forming a dynamical system of coupled equations for each grid cell. The design of the finite volume grid will be discussed in a later section.

FINITE VOLUME FLUX-STORAGE RELATIONSHIPS

Having defined the conservation equations for a finite volume, we now turn to the problem of identifying the average state variables and boundary fluxes within the volume. Although the finite volume method offers a simple and computationally efficient representation for water budgets, the particular form and relationship of the inputs, outputs, states and physical parameters must be made explicit if the approach is to go beyond traditional lumped models. In this section the local form of the average equations are developed.

Vertical Unsaturated Flow to/from a Water Table

A discrete approximation to the cell volume-average for soil moisture storage and vertical flow (5) has the integral conservation equation for each grid cell:

$$\sigma \frac{d\zeta}{dt} = q^{+} - q^{o} . \qquad (7)$$

The overbars are dropped for convenience. The forcing, q^{+} represents the various land-surface flux terms which are discussed later. An approximate expression is derived next to demonstrate how the flux at the water table q^{o} is an explicit a function of the cell average moisture storage $\overline{\zeta}$, and the relative position of the water table below the land surface, $z_s - \overline{\phi}$. The approximation is found by integration of the local equations for steady, vertical, unsaturated flow to a water table

$$q = -K(\psi)(1 + \frac{\partial \psi}{\partial z}) \qquad (8)$$

with $K(\psi)$ the hydraulic conductivity, a function of capillary pressure head ψ (taken to be negative). Substitution of (8) into the conservation equation yields the steady-state version of Richard's equation (1931):

$$\frac{\partial}{\partial z}(K(\psi)(1 + \frac{\partial \psi}{\partial z}) = 0 \qquad (9)$$

An exponential form for $K(\psi)$ is convenient here

$$\begin{aligned} K(\psi) &= K_s e^{\alpha(\psi - \psi_a)}; \psi \le \psi_a \\ &= K_s ; \ \psi \le \psi_a \end{aligned} \qquad (10)$$

where K_s $[LT^{-1}]$ is the hydraulic conductivity at saturation, ψ_a $[L]$ is a fitting parameter near the air-entry value of capillary tension in the soil; and α $[L^{-1}]$ is the soil texture parameter which determines the relative importance of gravity and capillarity for a given porous media (e.g. small α indicates a fine texture and large α a coarse texture soil). Using (9) and (10), and applying the Kirchoff transformation (Tindall and Kunkel, 1999), a solution to the vertical distribution $\psi(z)$ is found to be:

$$\psi(z) - \psi_a = \frac{1}{\alpha} Log\left[-\frac{q}{K_s} + \frac{K_s + q}{K_s} e^{-\alpha z} \right] \qquad (11)$$

where *z* is the height above the water table (+ upward). Note that constant vertical flux *q* is negative for infiltration and recharge to the water table, and positive for upward exfiltration and evapotranspiration from the water table. An expression for soil saturation *S*(*z*) and moisture content $\theta(z)$ can be expressed:

$$S(z) = \frac{\theta(z) - \theta_r}{\theta_s - \theta_r} = e^{\alpha(\psi - \psi_a)}; \psi \le \psi_a \quad (12)$$

Combining (11) with (12) leads to a form of the solution in terms of the distribution of saturation $S(z)$ or moisture content $\theta(z)$ above the water table

$$S(z) = -\frac{q}{K_s} + \frac{K_s + q}{K_s} e^{-\alpha z} \quad (13)$$

Integrating $S(z)$ over the vadose zone ($0 \le z \le z_s - \bar{\phi}$) and evaluating the flux at the water table or lower boundary of the vadose zone, $q = q^o$ yields:

$$\zeta(\phi) = S \cdot (z_s - \phi) = \int_0^{(z_s - \phi)} \frac{\theta(z) - \theta_r}{\theta_s - \theta_r} dz =$$

$$\left[\frac{1}{\alpha} (1 + \frac{q^o}{K_s})(1 - e^{-\alpha(z_s - \phi)}) - \frac{q^o}{K_s}(z_s - \phi) \right] \quad (14)$$

where S is the average soil saturation above the water table. Equation (14) explicitly represents how soil-moisture storage and depth to water table are functions of the steady-state vertical recharge or upward flux to/from the water table ($\mp q^o$) and the soil characteristics (K_s, α).

Figure 4 illustrates the relation (14) for a clay soil over a range of vertical flow rates, $\pm q^o$. Figures 5 illustrates the soil moisture-water table relation for a loam soil. For both soil types, under conditions of recharge ($q^o <$ 0), as the water table or saturated thickness increases over the flow depth from 0-20 m, the net unsaturated storage is reduced as the groundwater occupies an increasing fraction of the total flow volume. This inverse relation was explained in an earlier paper (Duffy, 1996) as a competition between the unsaturated and saturated states for the flow volume, and demonstrates the important control that the water table exerts on the moisture profile and vertical flux. For vertical upward flow ($q^o >$ 0), we observe an explicit storage deficit w/re to the neutral case (q^o = 0). Note that ζ, ϕ are positively correlated below a critical value of storage. As the water table increases the soil moisture storage increases, goes through a maximum and then decreases as $\bar{\phi} \to z_s$. For $q^o \ge 0$, the soil moisture storage evolves as a function of water table depth. As the water table approaches the land surface, the upward flux is only limited by the atmospheric conditions, while a deeper water table demonstrates the transition to soil-control on the upward flux.

The idea that the water table depth plays a important role in the dynamics of evapotranspiration was examined by Gardner in (1963). Rearranging (14) provides an explicit definition of the net flux at the water table q^o or recharge, in terms of the volume-averaged states $\bar{\zeta}$ and $\bar{\phi}$:

$$q^o(\zeta, \phi) = \frac{K_s \left(1 - e^{-\alpha(z_s - \phi)} - \alpha\zeta\right)}{\alpha(z_s - \phi) - (1 - e^{-\alpha(z_s - \phi)})} \quad (15)$$

Note that a singularity exists in (15) as $\phi \to z_s$, and this will need to be accounted for in applications by including a small constant. Figure (6) illustrates $q^o = f(\bar{\zeta}, \bar{\phi})$ for a clay-loam soil and a 10m depth to bedrock. From Figures (4-6) it is clear that the depth of the water table plays a crucial role in the vertical flux, and influences the the potential for recharge to, or evaporation from the water table. Equation (15) provides an explicit approximation for recharge at the water table as a function of the cell average unsaturated-saturated storage in the dynamical water balance model.

Saturated Unconfined Horizontal Flow

The local relation of the lateral or horizontal flow to the volume average saturated thickness is determined next. The dynamical model (5) for the saturated, horizontal flow component, is written:

$$\sigma \frac{d\phi}{dt} = q^o + \int_{\Gamma_i} (\phi - z_b) q \cdot \eta d\Gamma \quad (16)$$

where Γ is the projection of the control volume and control volume boundary in the horizontal plane. We note that q^o is the net rate of flux at the water table for projected area A_i. For a volume element (Fig. 3), the horizontal

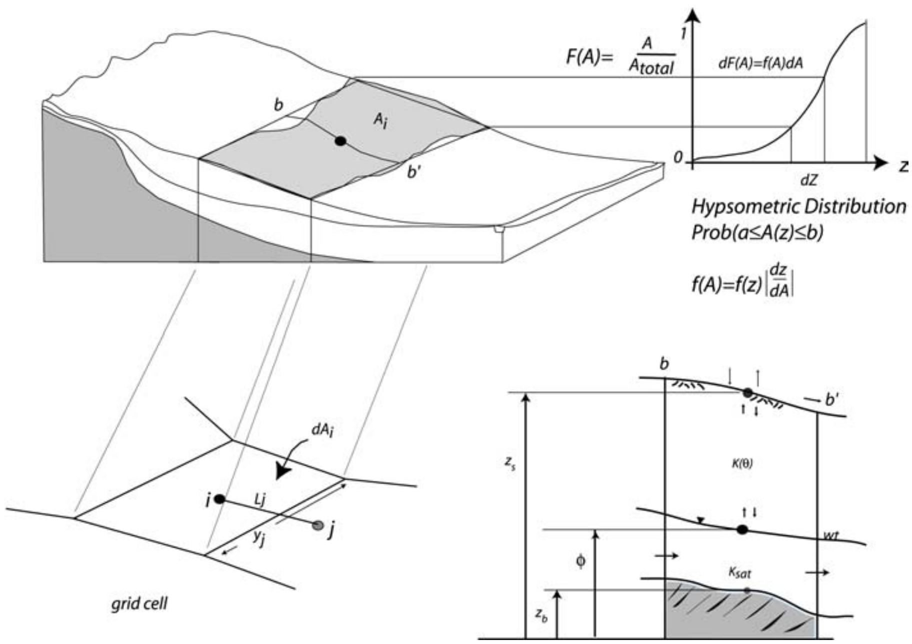

Figure 3. The topographic boundaries and hypsometric distribution used to delineate "similarity zones" and the major grid-cells for the dynamical model.

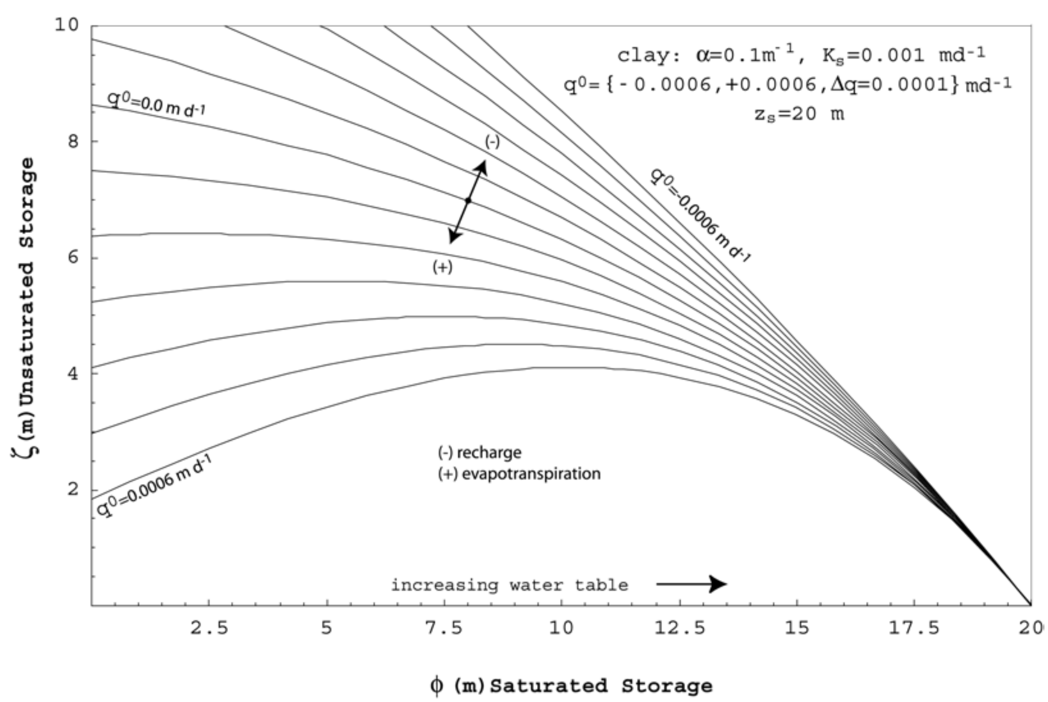

Figure 4. Theoretical saturated-unsaturated storage for a 20m clay layer based in eq. (14). The effect of recharge and evapotranspiration on storage above and below the water table is indicated.

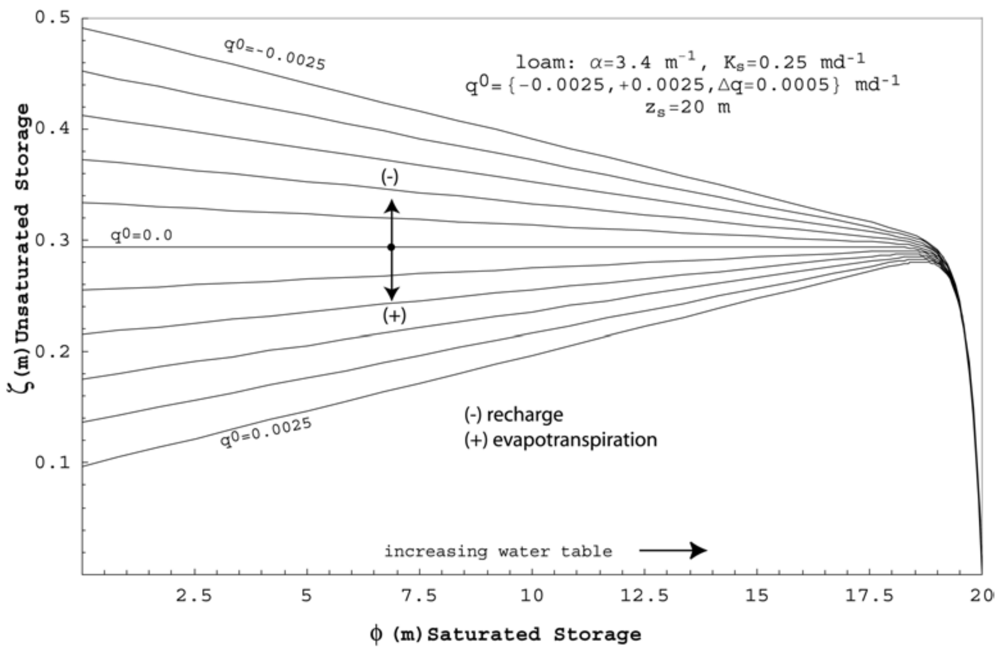

Figure 5. Theoretical saturated-unsaturated storage for a 20m loam soil layer based in eq. (14). The effect of recharge and evapotranspiration on storage above and below the water table is indicated.

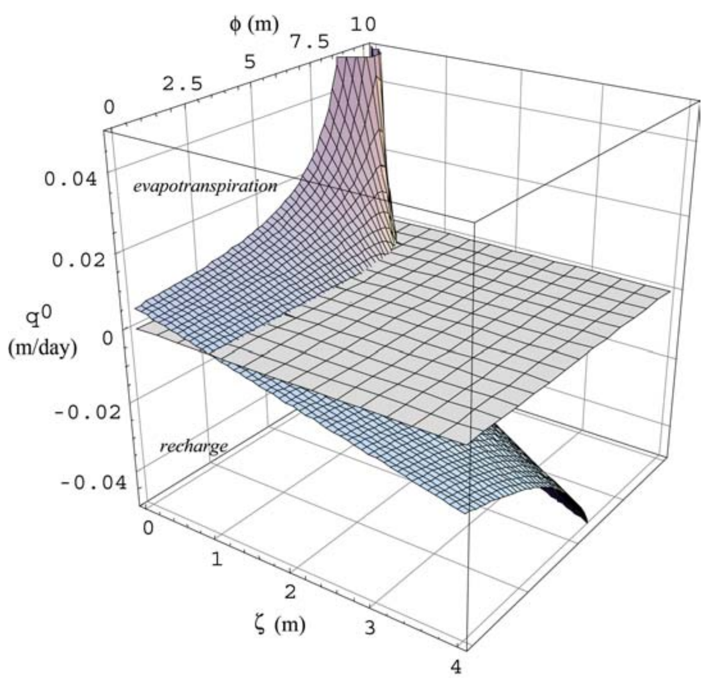

Figure 6. Theoretical relationship for the net flux (+/-) at the water table plotted versus saturated and unsaturated storage. The soil type is clay-loam and the soil thickness is 10 m. The plane of zero-flux is indicated.

flux Q_i / A_i per unit surface area separating the face connecting the *i-j* elements is defined by the Darcy equation:

$$\begin{aligned} \frac{Q_i}{A_i} &= q_i^- \\ &= -\tilde{K}_j(\phi_i - z_{b_i})\frac{y_j}{A_i l_j}(\phi_i - \phi_j) \end{aligned} \quad (17)$$

where q_i^- again is the volumetric flow per unit surface area of cell *i*; $\phi_i - z_{b_i}$ is the average saturated thickness; l_j is the horizontal distance between the *i-j* elements; y_j is the length of the adjoining sides of the *i-j* grid cell; $\tilde{K}_j$ is the average saturated hydraulic conductivity for *i-j* face of the grid cell:

$$\tilde{K}_j = \frac{K_i + K_j}{2} \quad (18)$$

Summing over all sides of element *i* yields the volume-averaged equation for saturated flow:

$$q_i^- = \sum_{j \in n(i)} \tilde{K}_j(\phi_i - z_{b_i})\frac{y_j}{A_i l_j}(\phi_i - \phi_j) \quad (19)$$

where the sum is over the *j* nearest neighbor cells *n*(*i*). To summarize, the subsurface flux terms within each grid cell for the semi-discrete dynamical model are:

$$q_i^+ = (p - e_t - q_r - q_s)_i \quad (20a)$$

$$q_i^0 = \left(\frac{K_s[1 - e^{-\alpha(z_s - \phi)} - \alpha\zeta}{\alpha(z_s - \phi) - (1 - e^{-\alpha(z_s - \phi)})} \right)_i \quad (20b)$$

$$q_i^- = \sum_{j \in n(i)} \tilde{K}_j(\phi_i - z_{b_i})\frac{y_j}{A_i l_j}(\phi_i - \phi_j) \quad (20c)$$

The components of q_i^+ in (20a) are the sum of precipitation (p), evapotranspiration (e_t), runoff from precipitation excess (q_r) and saturation overland flow (q_s). These are discussed in a later section.

STREAM BOUNDARY CONDITIONS

In the case where an element is bounded by a perennial or ephemeral stream, the flux expression (20c) must be altered to admit the proper boundary condition. Figure 7a illustrates a perennial stream where ϕ_c is the channel stage, above stream bed elevation z_c , and the distance from the element node to the channel is l_j. The perennial channel is assumed to be narrow in this formulation ($w_c << l_j$). Lateral flow per unit surface area q^- in (20c), with the modification to incorporate a perennial channel on the side y_j, is given by:

$$q_i^- = -\tilde{K}_j(\phi_i - z_{b_i})\frac{y_j}{A_i l_j}(\phi_i - \phi_{c_j}) \quad (21)$$

Ephemeral streams or arroyos require a separate approach as the water table is below the streambed (Figure 7b) and stream losses contribute to the unsaturated zone. For simplicity we again assume the channel to be narrow ($w_c << l_j$). The loss in the channel per unit surface area to grid cell *i* (or *j*) is given by:

$$q_{c_i}^+ = \left(\gamma \frac{Q_c}{2A} \right)_i, \quad Q_{c_i} = (y w_c u_c)_i \quad (22)$$

where the channel volumetric flow is Q_c, and γ is the loss fraction. The length, width and average velocity of the channel are $y, w_c,$ and u_c respectively. Note that the channel loss for the line source partitions infiltration equally to the adjacent subsurface elements, *i* and *j*. It is straightforward to extend this simplified boundary condition to wide channels, where an explicit channel grid cell would be included.

Since 1970, considerable research has shown that within the flood plain of perennial channels, saturation overland flow or rejected rainfall can become an important runoff mechanism (e.g. Dunne and Black, 1970). This is sometimes referred to as “partial-area” runoff. During rain events the shal-
low water table quickly saturates the surface area near the channel. From the perspective of a dynamic balance, q_s represents a negative feedback mechanism for infiltration (Duffy, 1996). The mechanism is explained as a water table rise near the channel during the infiltration event. As the event continues, the satu

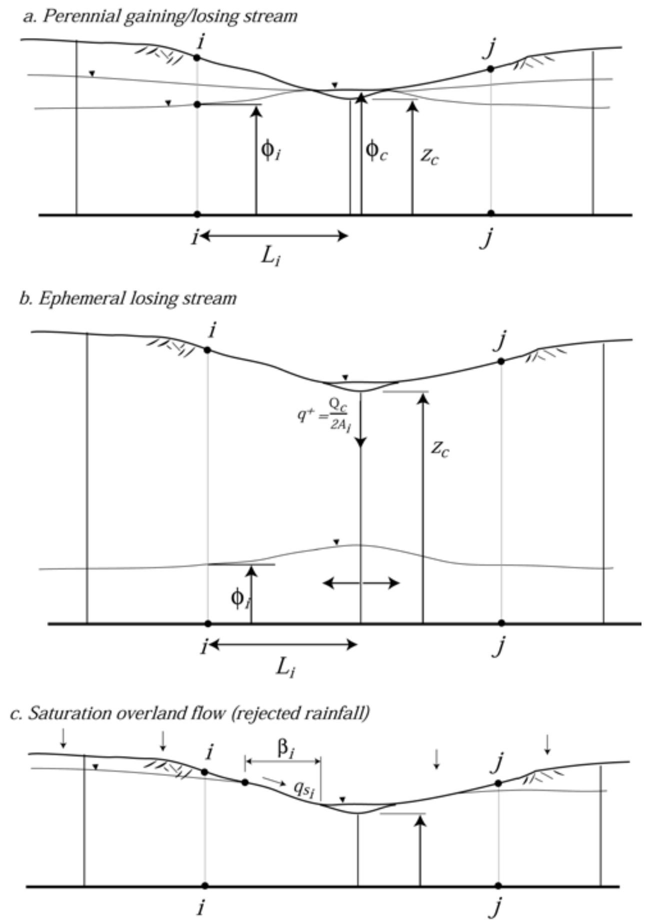

Figure 7. Boundary conditions for a) the perennial stream, b) the ephemeral stream, c) the saturation overland flow region near the channel.

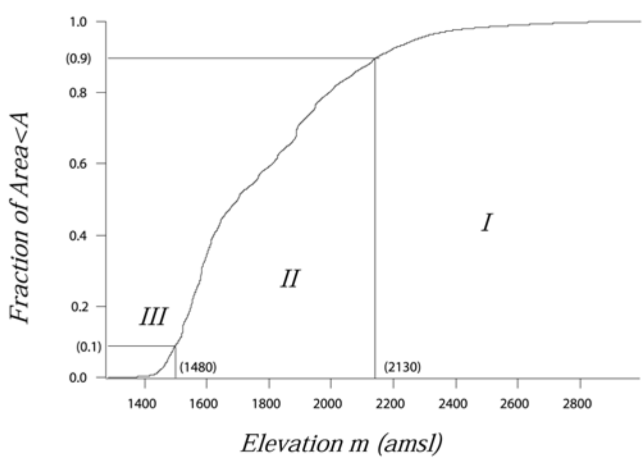

Figure 8. The hypsometric function for the Llano de Sandia (Figure 1), and the delineated area-elevation for the similarity zones of the conceptual model (Figure 2).

rated surface-area near the channel grows in area (e.g. partial-area concept). This growth in saturated area, limits the net area which can allow infiltration, causing saturation overland flow (rejected rainfall). Taken together this constitutes a negative feedback effect on infiltration and recharge. Duffy et al (1994) have shown that runoff from rejected rainfall or saturation overland flow from the partial area can be expressed as:

$$q_s = \beta p; \quad \beta(\phi) = b(\phi - \phi_c) \tag{23}$$

where *p* is precipitation; $\beta(\phi)$ is the saturated fractional area of an grid cell, and *b* is a fitting parameter (Fig 7c). The feedback concept is easy to see by combining q_s, q_r and *p* into net infiltration at each grid cell adjacent to a perennial channel,

$$\begin{aligned} q_i^+ &= (p - q_s - q_r)_i \\ &= (1-\beta_i)p_i; \quad p_i < K_i \\ &= (1-\beta_i)K_i; \quad p_i \geq K_i \end{aligned} \tag{24}$$

where K_i is the unsaturated conductivity of the soil. Equation (24) shows that for low rates of precipitation $p_i < K_i$, infiltration will cause the water table to rise near the stream. As the near-stream ground becomes saturated, rainfall is rejected. Infiltration q_i^+ is limited to the upslope parts of the element within the area fraction, $1-\beta_i$. For high rainfall rates $p_i \geq K_i$, infiltration also occurs as Hortonian runoff or precipitation excess

$$(q_r)_i = (1-\beta)(p_i - K_i).$$

SHALLOW WATER TABLE APPROXIMATION

In the riparian region bordering the Rio Grande, our conceptual model suggests a shallow water table (< 2 m) and the potential for significant evaporation and transpiration directly from the water table. In general the upward flux is a function of the unsaturated and the saturated zone as demonstrated in Figures (4-6). However, in the shallow water table case, a simplification of the model is possible. From the dynamical systems perspective, Haken (1978) tells us that under conditions where a wide separation in time scales exists, a slowly varying state may control the evolution of fast variable in a way that effectively reduces the dimension of the state space. This is sometimes referred to as the "enslaving principal". In Figures (4-6), we see that when $\phi \to z_s$ all curves tend to the $q^o = 0$ result suggesting $\zeta(\phi)$ in (14) may be independent of q^o for shallow water table conditions. By writing the 2-state model (5) in terms of total water storage in the finite volume $(\zeta + \phi)$ and simplifying, we eliminate q^o. The model for the time rate of change of the total storage is:

$$\sigma \frac{d}{dt}(\zeta + \phi) = q^+ - q^- \tag{25}$$

Expanding $\zeta(\phi)$ in (25) yields

$$\sigma\left(\frac{d\zeta}{d\phi}\frac{d\phi}{dt} + \frac{d\phi}{dt}\right) = q^+ - q^- \tag{26}$$

Evaluation of $d\zeta / d\phi$ from (14) and simplifying gives a reduced model for shallow water-table condition

$$\begin{aligned} \sigma(\phi)\frac{d\phi}{dt} &= q^+ - q^- \\ \zeta(\phi) &= \frac{1}{\alpha}\left(1 - e^{-\alpha(z_s - \phi)}\right) \end{aligned} \tag{27}$$

Thus for shallow water table conditions, we see that the dynamical model reduces to a single differential equation for saturated flow, with an algebraic relation for soil moisture storage (e.g. a differential algebraic equation). The soil moisture ζ becomes an exponential function of depth to water. The storage coefficient $\sigma(\phi)$ in this case is redefined to be function of the water table depth as well:

$$\sigma(\phi) = (\theta_s - \theta_r)\left(1 - e^{-\alpha(z_s - \phi)}\right) \tag{28}$$

The variable storage coefficient has the limits

$$\begin{aligned} \sigma(\phi) &\to 0, \phi \to z_s \\ \sigma(\phi) &\to (\theta_s - \theta_r),\ \phi \to 0. \end{aligned}$$

Bierkens (1998) also has derived a dynamic model for shallow, saturated groundwater flow similar to (27), using the Van Genuchten-type soil properties (1980). It is shown here that (27) is a special case of the 2-state storage model for shallow water table conditions (Duffy, 1996). Application of this form of the model requires a large separation in the time scale for the master (ϕ) and slave (ζ) states. Practically speaking, for the examples of Figures 4-6, this amounts to water table depths in the range of 0-5 meters below the surface.

EVAPOTRANSPIRATION

Evapotranspiration is a function of both the unsaturated and saturated state variables. Although there are many possible relationships, here the Thornthwaite and Mather (1955) relationship is used for e_t, which is defined as the product of a vegetation coefficient c, potential evaporation e_p and a function of the average saturation S:

$$\begin{aligned} e_t &= c\, e_p f; \quad S_o \le S \le S_{fc} \\ e_t &= c\, e_p; \quad S > S_{fc} \\ f &= f(S) = \frac{S - S_o}{S_{fc} - S_o}; \\ S &= \frac{\zeta}{z_s - \phi} \end{aligned} \tag{29}$$

The average saturation S is defined in (29), and $f(S)$ is the relative saturation, depending on the water table and the depth of moisture in the unsaturated zone. S_o is the average saturation as $z_s - \phi \to \infty$ and at the minimum upward flux rate (e.g. wilting point conditions), and S_{fc} is the average saturation at field capacity for $|q| = 0$. The vegetation coefficient c is determined from Jensen (1973) or other models representing the vegetation type and stage of growth.

SNOWMELT

Snowmelt is a major component of runoff and water supply in the Rio Grande. A dynamical equation for accumulation and melt of the snowpack on a grid cell is given by Dingman (1994):

$$\left[\frac{d\xi}{dt} = p - e_s - m_s\right] A_i, \tag{30}$$

The average snow water equivalent depth is defined for the grid cell as:

$$\xi_i = \frac{a_s \rho_s}{A_i} \int_{A_i} h_s dA \tag{31}$$

where h_s is snow depth, ρ_s is snow density, b_s and a_s are coefficients. The snowmelt rate m_s is defined in terms of the air temperature T_a and the average snow temperature T_s:

$$m_s = \begin{cases} b_s(T_a - T_s); & T_a > T_s \\ 0; \quad T_a \le T_s \end{cases} \tag{32}$$

Derivation of a physically-based model including a complete energy balance and humidity conditions for evaporation of snow (e_s) is currently under development (Qu and Duffy, 2004).

MOUNTAIN-FRONT RECHARGE

Finally, we demonstrate the model for estimating mountain-front recharge at the Llano de Sandia site. Figure 3 illustrates the hydrologic conceptual model discussed earlier in this paper, and specifies three dominant zones based on similar climate, hydrology and vegetation: 1) Upland shallow soils over deep fractured bedrock, 2) Bajada, alluvial fan and, 3) Flood plain and riparian river corridor. The hypsometric function, shown in Figure 8, quantifies the area-elevation for the region, and the fractional area of the 3 zones is indicated. In this example, where strong elevation gradients dominate the hydroclimatic and vegetative changes, the distribution of area with elevation (area < *A(z)*) captures the dominant controls on recharge for this landscape . It is worthwhile to mention that the concept of a *Conceptual Hydrologic Landscape*, recently reviewed by Tom Winters (2001), is a useful strategy for classification and conceptualization of the coupling of surface and groundwater relationships in different terrain types. As stated by Winters (2001), "..the conceptual framework can then be used to develop hypotheses of how the hydrologic system might function in those terrains."

We should also note that the classification is based on a similarity condition among terrain features, geology, vegetation, climate and soil patterns. With this in mind, the mountain-front model to be developed next, may have wider applications to similar physiographic and hydroclimatic conditions of the Basin and Range in the western US.

Next we build the coupled surface-subsurface coupled water balance model for the region. In this example, we focus on the subsurface-surface coupling and the longer time scales associated with mountain-front recharge. In this example the upland mountain region is treated as shallow "leaky" aquifer (zone 0) overlying a deep bedrock system (zone 1). The alluvial fan (zone 2) and the Rio Grande corridor (zone 3) complete the coupled model regions.

The fully-coupled water balance model is given by:

$$\begin{cases} \sigma_0 \dot{\zeta}_0 = q_0^+ - q_0^o \\ \sigma_0 \dot{\phi}_0 = q_0^o - q_0^- - q_0^l \\ \sigma_1 \dot{\zeta}_1 = q_0^l - q_1^o \\ \sigma_1 \dot{\phi}_1 = q_1^o - q_1^- \\ \sigma_2 \dot{\zeta}_2 = q_2^+ - q_2^o \\ \sigma_2 \dot{\phi}_2 = q_2^o + \dfrac{A_1}{A_2} q_1^- + \dfrac{A_1}{A_2} q_0^- - q_2^- \\ \sigma_3 \dot{\zeta}_3 = q_3^+ - q_3^o \\ \sigma_3 \dot{\phi}_3 = q_3^o + \dfrac{A_2}{A_3} q_2^- - q_3^- \end{cases} \quad (33)$$

where the superscripts on the flux terms identified in (20) represent infiltration (+), recharge (0), lateral flux (-) or baseflow, and a leakage (l). Note that zone (2) receives lateral flow from zone (1) q_1^- and it is assumed that runoff from the upland zone q_0^- entirely infiltrates in the ephemeral channels of zone (2). The groundwater discharge from the upland shallow system and baseflow flux to/from the Rio Grande are respectively:

$$q_0^- = -K_0(\phi_0 - z_{b_0}) \frac{y_0}{A_0 l_0} (\phi_0 - z_{l_0})$$

$$q_3^- = -K_3(\phi_3 - z_{b_3}) \frac{y_3}{A_3 l_3} (\phi_3 - \phi_{c_3})$$

The leakage from zone (0) to (1) is:

$$q_0^l = -\frac{K_l}{d_l} (\phi_0 - z_{l_0})$$

where K_l is the hydraulic conductivity of the leaky layer, d_l is the thickness, and z_l is the average elevation of the layer. The remaining equations have the general form of (20a,b,c). Beyond the physiographic and geometric support required to solve the above system, the corresponding parameters associated with each region must be identified. Table 1. gives crude estimates of the parameters for each zone in the model.

Abrupt Climate Change Scenario

In order to demonstrate the significance of the coupled water budgets across altitude changes of the Llano de Sandia, a climate variation scenario was developed where the upland forcing (recharge) was abruptly reduced from 0.0005 to 0.00025 md^{-1}, 50 years into the simulation. Estimates of recharge rates were given by Anderholm (2000) to be in the range of 0.7 to 21% of mean annual precipitation, and these were used to estimate the recharge for the upland zone. For

The entire simulation the river corridor was assumed to have a constant average loss from evapotranspiration of 0.0006 md^{-1}. The conceptual model suggests that the alluvial fan receives little or no diffuse recharge ($p<<e_t$). However, the model does allow ephemeral channel recharge due to upland runoff from zone (0) to occur. The critical question to be answered by the abrupt climate scenario is: What is the relation of mountain-front recharge and riparian discharge on the net gain or loss to the Rio Grande? The model (33) was solved using Mathematica for the conditions described above, and the resulting fluxes are summarized in Figure 9. We first note that the mountain block fracture flow zone has the most dynamic response of the 3 deep groundwater zones during and after the wet-to-dry transition. The

shallow upland zone (0) simply follows the transition producing rapid deep leakage to zone (1) and runoff to zone (2). The alluvial fan zone (2), or transmission zone, represents 80% of the area of the system and is characterized by a very long time scale. The flux through zone (2) slowly decreases through the entire 200+ years of the simulation. The net discharge to the Rio Grande in zone (3) shows a dynamic but long term response, with increasing positive baseflow to the Rio Grande through the early wet climate interval (0-50 yr); and a gradual decline and flow reversal at ~100 years. That is, the Rio Grande looses flow to the adjacent groundwater during the later years of the simulation. There is insufficient upland recharge to maintain baseflow.

For a second application, the local effect of dynamic forcing on soil moisture, shallow water table fluctuations and stream depletion was examined. The forcing is specified by simulated daily precipitation and potential evapotranspiration. Equation (29) was used for the soil moisture effect on e_t. The model is formed within the upland recharge and alluvial fan set to zero flux. The results for 3 years of daily climate forcing is illustrated in Fig. 10. Figure 10, demonstrates that for shallow water table conditions, the mean soil moisture state simply "follows" the water table fluctuations. That is, the relatively long time-scale of groundwater flow "enslaves" the soil moisture in this case (see text). The riparian dynamic model indicates that the ultimate source of e_t in this example is stream depletion. Apparently, over long periods of time, e_t from the water table induces stream losses. The depletion is indicated by $\phi < \phi_c$ in Figure 10. It is also interesting that precipitation (<25 cm/yr) has almost no effect on the result as $e_t \approx q^-$ and given the large potential evapotranspiration. However, it is important to note that this example does not necessarily imply that the plants are the only or the primary cause of this depletion. Clearly the shallow water table in this case would a have significant direct component of evaporation from soil moisture and the water table, in addition to transpiration. This suggests the need for a more careful partitioning of transpiration and vegetation dynamics.

SUMMARY AND CONCLUSIONS

This research attempts to develop a physical basis for a discrete dynamical water balance model appropriate for large-scale river basins such such as the Rio Grande. The model discretization uses the natural coordinates of the terrain to delineate spatial elements. The conceptual model approach outlined here, uses qualitative characteristics of the hydrology, climate and vegetation to further decide on the scale or dimension of the dynamical model and the coupling of major storage features across the landscape. Over the longer term this research is attempting to understand, through dynamical model

simulation and parameter estimation, the impacts of long term climate and landuse effects on water resources, and to provide a relatively simple yet physically-based approach to long range water resource forecasting.

Acknowledgments. This research was funded by grants to the author from the National Science Foundation: 1) Science & Technology Center for Sustainability of Water Resources in Semi-Arid Regions (NSF EAR 9876800, L.D. James), and 2) NASA (ER020059) The Role of Soil Moisture & Water Table Dynamics in Ungaged Runoff Prediction in Mountain-Front Systems (NASA_GAPP Program, J. Entin). This support is kindly acknowledged. The author would also like to thank Everett Springer and Brent Newman of Los Alamos National Laboratory for their support of this research effort during the summers of 1999-2001.

REFERENCES

Anderholm, S. 2000, Mountain-Front Recharge along the eastern side of the Middle Rio Grande Basin, central New Mexico, USGS WRI-2000-4010, 36p.

Bierkens, M. 1998, modeling water table fluctuations by means of a stochastic differential equation, Water Resources Research, 34(10), 2485-2499.

Duffy, C. J., D. H. Lee and M. Jin, 1994. Dynamics of soil moisture, subsurface flow and runoff in complex terrain, Environmental Resources Research Institute, Penn State University, University Park. 95 pp.

Duffy, C.J., A two-state integral-balance model for soil moisture and groundwater dynamics in complex terrain, Water Resources Research, 32(8), 2421-2434, 1996.

Dunne, T and R. Black, 1970, Partial-area contributions to storm runoff in a small New England watershed, Water Resources Research 6:1296-1311.

Haken, H. 1978. Synergetics, An Introduction, 2nd ed. Springer Verlag.13Jakeman A. J. and G. M. Hornberger, How much complexity is warranted in a rainfall runoff model, Water Resour. Res., 29(8), 2637-2649, 1993

Muldavin, E., G. Shore, K. Taugher, and B. Milne. 1998. A Vegetation Classification and Map for the Sevilleta National Wildlife Refuge, New Mexico: Final Report: University of New Mexico, Biology Department, Albuquerque, NM. , 45pp.

Qu, Y. and C. J. Duffy, 2004, A GIS-Based, semi-discrete model for multi-scale water budgets. To be submitted, Journal of Hydrology.

Richards, L.A., Capillary conduction of liquids through porous mediums, Physics, 1, 318-333, 1931.

Spiegel, Z. 1955, Geology and Ground-Water resources of Northeastern Socorro, County,NM. Groundwater Report 4: State Bureau of Mines and Mineral Resources, NMIMT,Socorro, NM. 99p.

Thornthwaite, C. W. 1948. An approach toward a rational classification of climate,Geographical Review, 38, p.55-94.

van Genuchten, M.Th., A closed-form equation for predicting the hydraulic conductivityof unsaturated soils, Soil Science Society of America Journal, 44, 892-898, 1980.

Walvoord, M. 2002, A unifying conceptual model to describe water, vapor, and solute transport in deep arid vadose zones. Ph.D. thesis, New Mexico Tech.

Weiss, J. , D. Gutzler, J. Coonrod, and C. Dahm, 2003, Seasonal and interannual relationships between vegetation and climate of central New Mexico, USA. Journal of Arid Environments, in press.

Winter, T. 2001. The Concept of Hydrologic Landscapes, Jour. of the American Water Resources Association. 37(2):335-349..

Civil and Environmental Engineering, Penn State University, University Park, PA 16802..

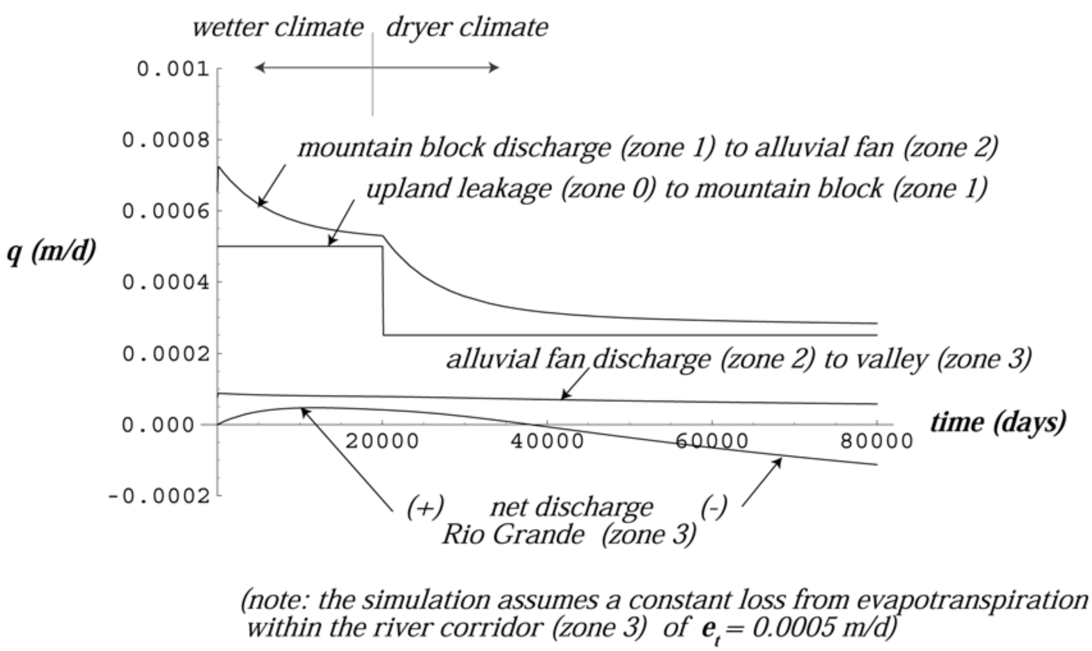

Figure 9. Abrupt climate-change simulation scenario for the coupled, long-term water budget for the Llano de Sandia in central New Mexico (Figure 1). The simulations (33) show the response of the 3 similarity zones undergoing an abrupt transition from wet to dry climate conditions 50 years into the simulation. The flux is given as volumetric flow rate per unit surface area. Note the long term impact on the Rio Grande is the eventual switching from a gaining stream to a losing stream. Evapotranspiration within riparian corridor is a major loss of water. This is held constant throughout the simulation. Also note that the transition occurs more than 50 years after the climate shift.

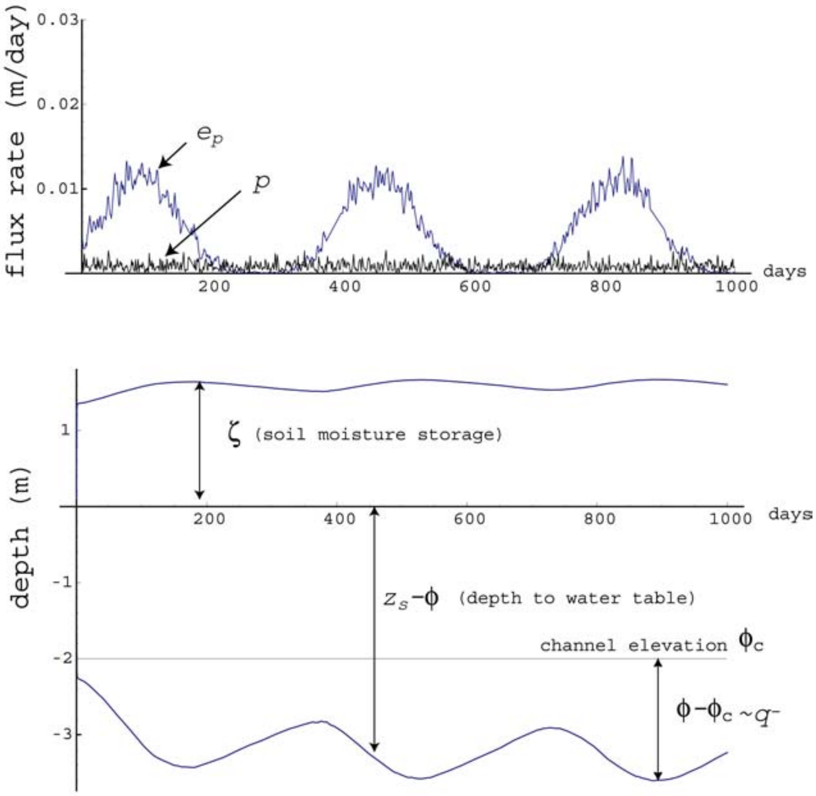

Figure 10. Results of the dynamical model (33) where zone 3 or the river corridor is active and zones 0-2 are turned off. The simulation illustrates dynamic precipitation and seasonal evapotranspiration forcing on the soil moisture storage and water table dynamics. Note that without upland recharge, the net effect of seasonal evapotranspiration is to create stream depletion.

Table 1. The parameters used in the Abrupt Climate Change Scenario model simulation (33). The parameter $\lambda_i = (AL/y)_i$ is estimated for each region using GIS.

Parameter	Zone 0	Zone 1	Zone 2	Zone 3
z_s (m)	997	800	400	55
ϕ_c (m)	800	–	200	50
recharge (md^{-1})	0.0005	–	0.0	-0.0006
K_s (md^{-1})	4	8	10	3
α (m^{-1})	2	1	1	1
σ (LL^{-1})	0.2	0.06	0.2	0.3
λ (L^2)	4.5×10^6	2.2×10^7	1.8×10^8	4.5×10^6
z_b (m)	800	0	0	0
$K_L d_L^{-1}$ (t^{-1})	0.4	–	–	–
ϕ (t=0)	801	100	90	50
ζ (t=0)	1	4	3	1

Short Title: Modeling Mountain-Front Recharge

AUTHOR NAMES

Semi-Discrete Dynamical Model for Mountain-Front Recharge and Water Balance Estimation

(Rio Grande of Southern Colorado and New Mexico)

Christopher J. Duffy[1]

Civil & Environmental Engineering Department, Penn State University, University Park, Pennsylvania